

**Cell Reports, Volume 29**

**Supplemental Information**

**Differential Functions of Splicing Factors  
in Mammary Transformation and  
Breast Cancer Metastasis**

**SungHee Park, Mattia Brugiolo, Martin Akerman, Shipra Das, Laura Urbanski, Adam Geier, Anil K. Kesarwani, Martin Fan, Nathan Leclair, Kuan-Ting Lin, Leo Hu, Ian Hua, Joshy George, Senthil K. Muthuswamy, Adrian R. Krainer, and Olga Anczuków**

SUPPLEMENTAL FIGURES

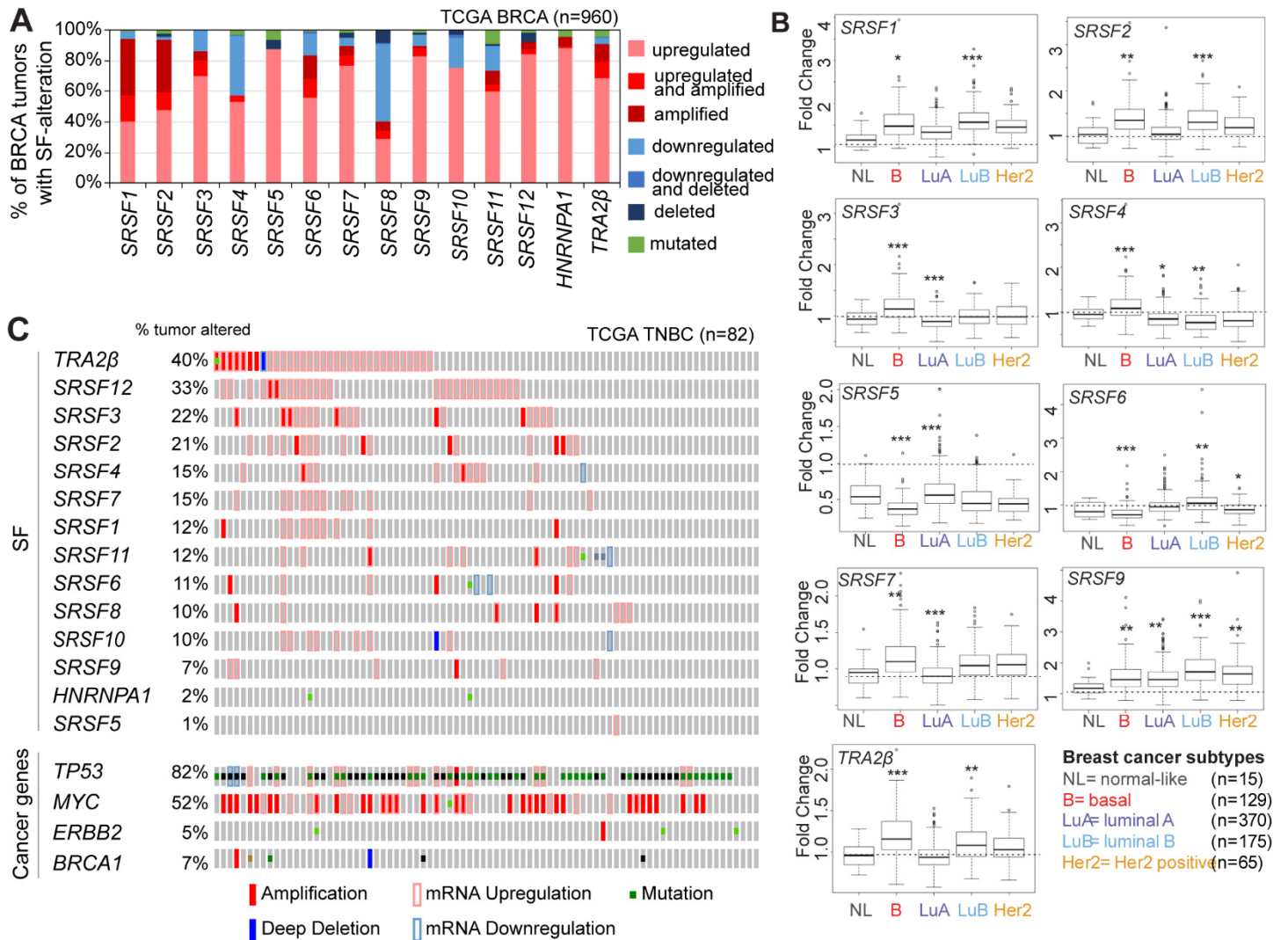


**Figure S1. SFs exhibit different alteration patterns in human breast tumors and are associated with different breast cancer subtypes** (related to Figure 1).

**(A)** Type of SF alterations detected in TCGA human breast tumors (n=960), normalized to total SF alterations for each gene. % of tumors that exhibit an alteration is shown for each of the following categories: i) mRNA upregulation (Z-score $\geq$ 2.0), ii) both mRNA upregulation and DNA amplification, iii) DNA amplification only, iv) mRNA downregulation (Z-score $\leq$ -2.0), v) both mRNA downregulation and DNA deletion, vi) DNA deletion only, and vi) mutation.

**(B)** SF expression in breast tumors classified into subtypes using the PAM50 signature is compared to ‘normal’ breast tissues (n=99). SF expression in each subtype is compared to the combination of all other subtypes (t-test; \*\*\* $P$ <1.10 $\cdot$ 10 $^{-10}$ , \*\* $P$ <0.00001, \* $P$ <0.01). Only SFs that exhibit differences between subtypes are shown.

**(C)** Graphical representation of SF alterations in TCGA TNBC (n=82). Copy number and expression changes are assessed by DNA- and RNA-seq. Individual genes are represented as rows, and individual patients as columns. Alterations in breast cancer genes *TP53*, *MYC*, *ERBB2* and *BRCA1* are in the lower panel.

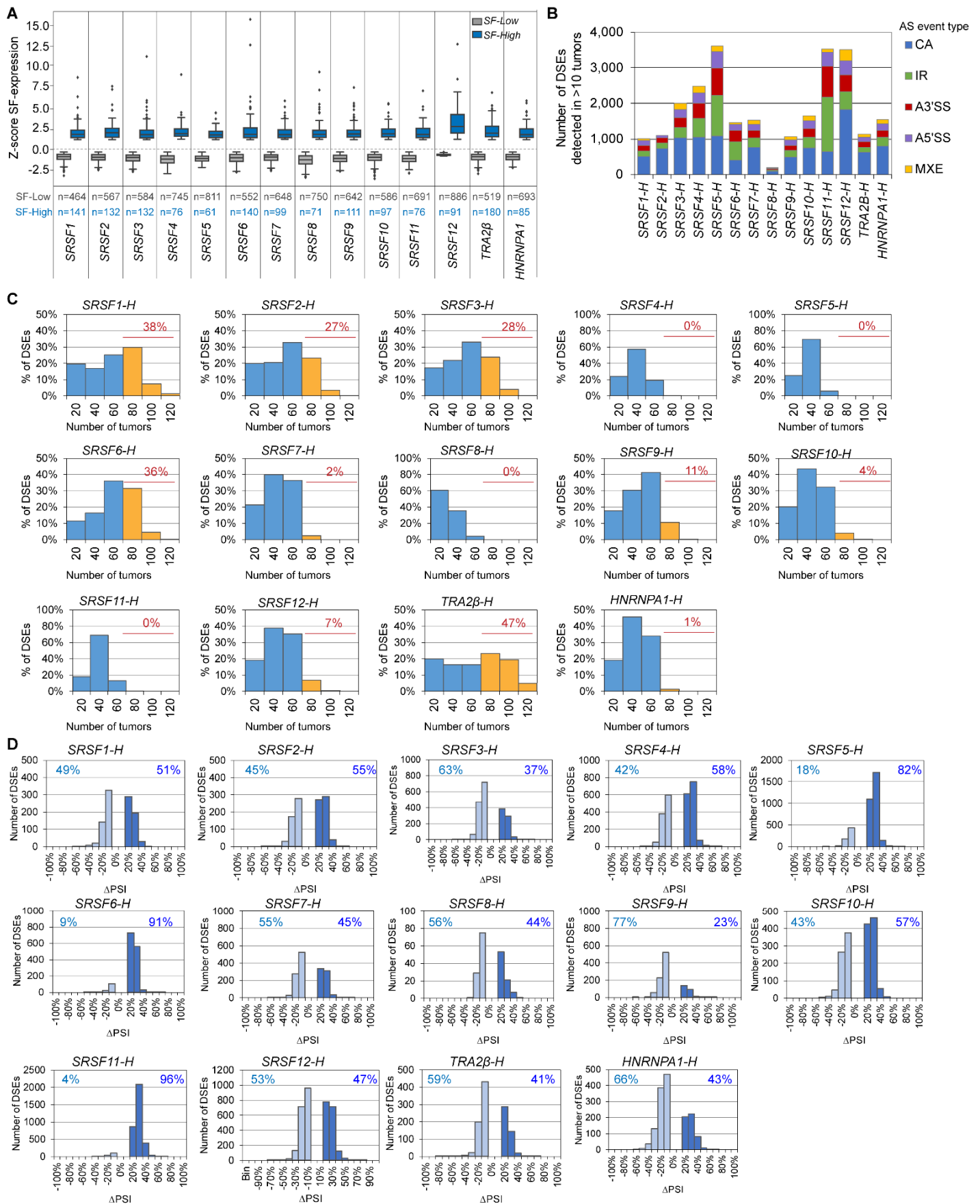


**Figure S2. TCGA breast tumors with high SF levels exhibit alterations in alternatively spliced isoforms (related to Figure 1).**  
**(A)** TCGA human breast tumors are classified based on *SF*-expression into two groups: *SF-high* ( $Z$ -score  $>1.5$ ) or *SF-low* ( $Z$ -score  $\leq 0$ ) for each listed SF. The number of samples in each category is indicated.

**(B)** Number of DSEs detected by RNA-seq in *SF-high* vs. *SF-low* TCGA breast tumors in at least 10 tumor samples ( $|\Delta\text{PSI}| \geq 10\%$ ;  $\text{FDR} < 5\%$ ;  $P < 0.01$ ) sorted by AS event type (CA: cassette exon; MXE: mutually exclusive exon; RI: retained intron; A5'SS: alternative 5' splice site; A3'SS -alternative 3' splice site).

**(C)** Number of *SF-high* tumor samples in which DSEs are detected, plotted for each SF. % of DSEs detected in  $\geq 80$  tumors is indicated.

**(D)** Skipped ( $\Delta\text{PSI} \leq -10\%$ ) and included ( $\Delta\text{PSI} \geq 10\%$ ) DSEs in *SF-high* vs. *SF-low* TCGA breast tumor samples reproducibly detected in  $\geq 10$  tumor samples were plotted by  $\Delta\text{PSI}$  values. % of skipped and included DSEs are indicated.

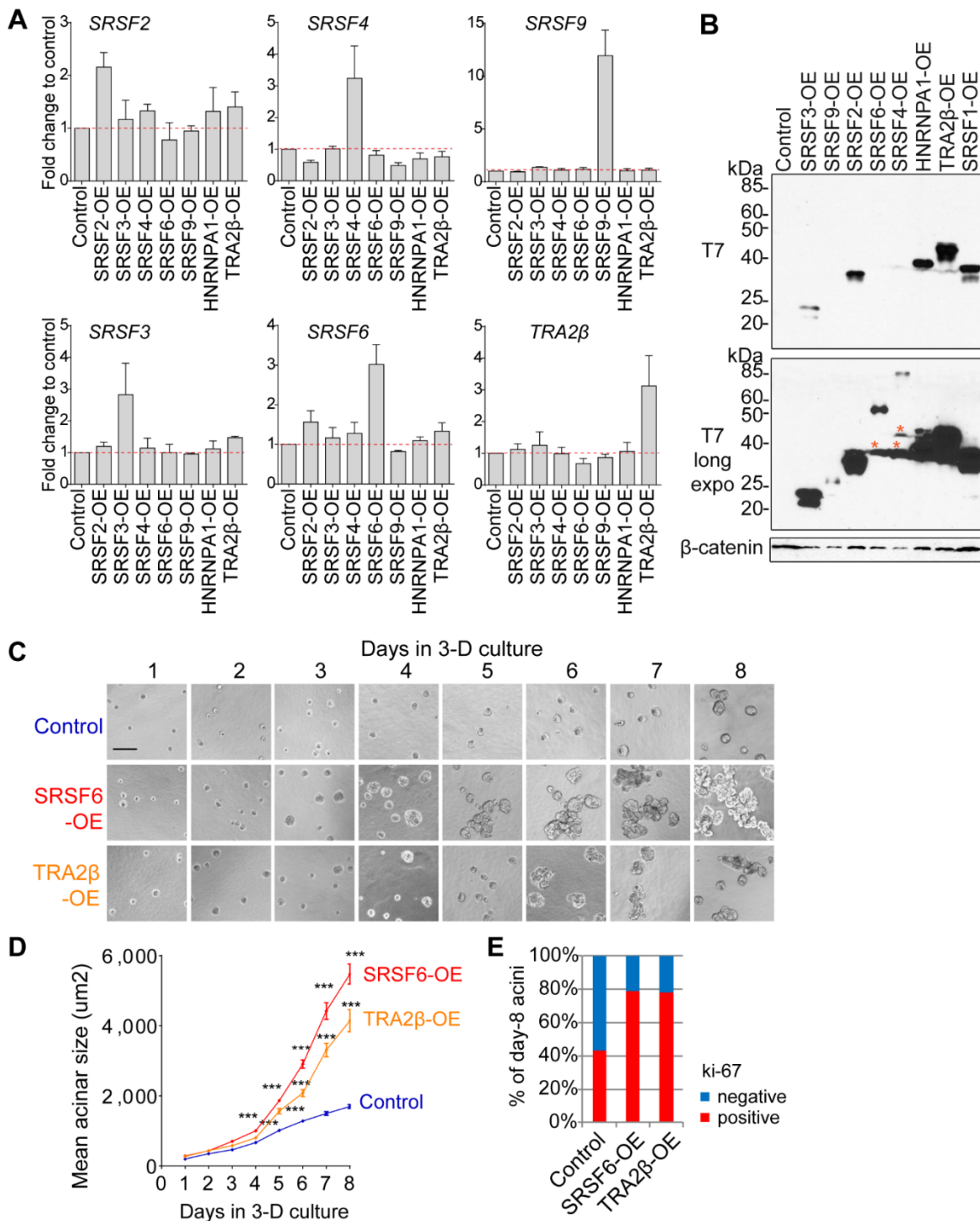


**Figure S3. Stable overexpression of specific SFs in human mammary epithelial MCF-10A cells promotes early changes in mammary acinar morphology, size and proliferation** (related to [Figure 2](#)).

(A) *SF* mRNA expression in SF-OE stable MCF-10A cell lines as measured by RT-QPCR using specific primers and normalized to control MCF-10A cells (n=3 biological replicates; mean±SD).

(B) Protein expression of T7-tagged SFs stably overexpressed in MCF-10A cells as detected by western blot using a T7 mouse antibody, with a  $\beta$ -catenin loading control. Stars indicate nonspecific bands on a longer exposure.

(C) Representative brightfield images of acini size and morphology in control and SF-OE MCF-10A cells from day 1 to 8 (Scale bar: 50  $\mu$ m).

(D) Acinar sizes of control and SF-OE acini from day 1 to 8 (n=3 biological replicates; >100 acini per experiment; Mann-Whitney \*\*\* $P$ <0.0001; mean±SD).

(E) Proliferation of control and SF-OE acini is assessed by immunostaining with a Ki-67 antibody quantified as % of Ki-67-positive in day-8 acini (n $\geq$ 3 biological replicates; >50 acini per experiment).

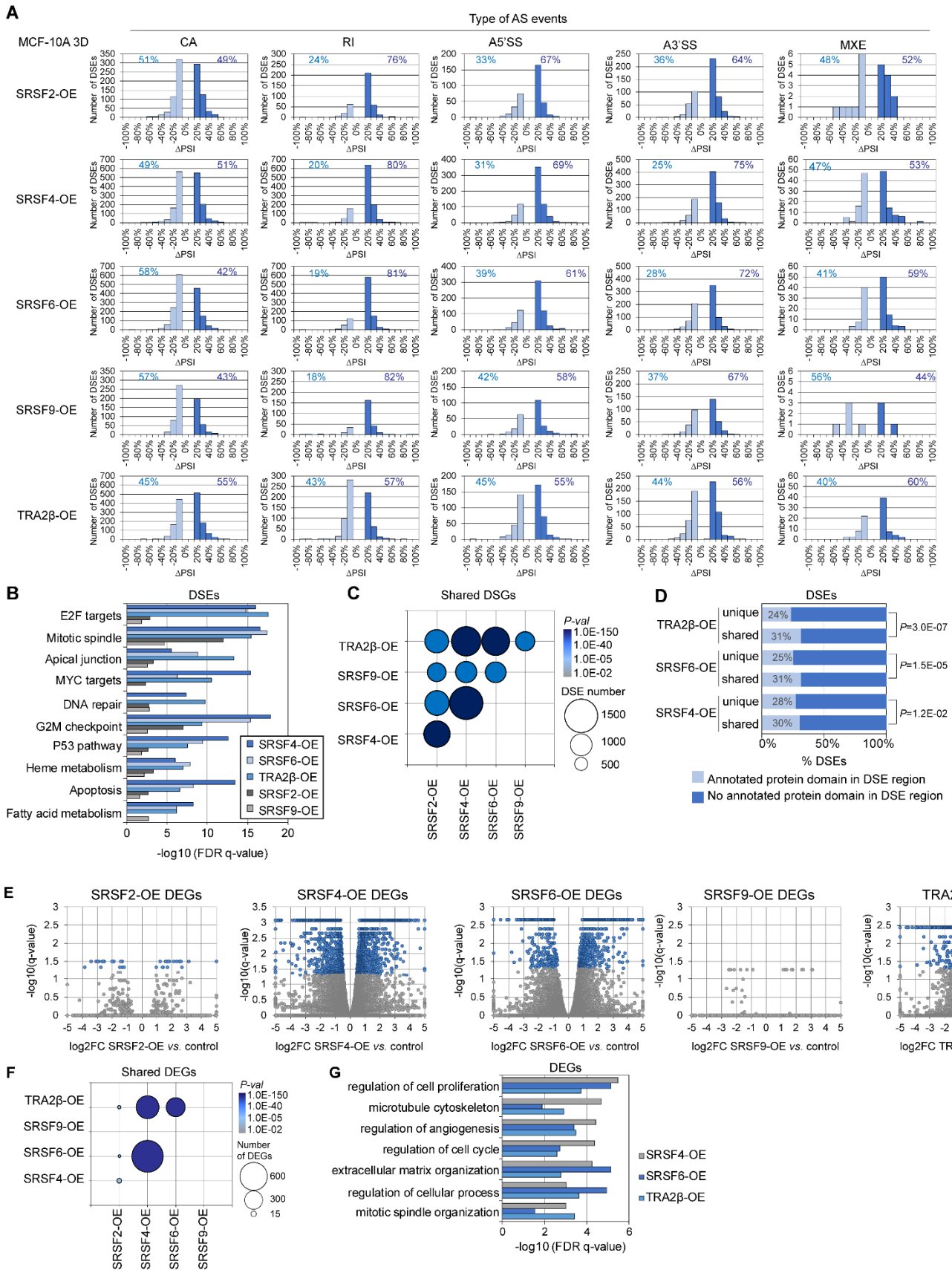


**Figure S4. SF-OE in human mammary MCF-10A cells leads to differential splicing and gene expression (related to Figure 3). (A-D) Similarities and differences in differentially spliced events (DSEs).**

- (A) Skipped ( $\Delta\text{PSI} \leq -10\%$ ) and included ( $\Delta\text{PSI} \geq 10\%$ ) DSEs in SF-OE vs. control MCF-10A day-8 acini plotted by  $\Delta\text{PSI}$  values for each SF and for each AS event type (CA: cassette exons; A3'SS: alternative 3' splice site; A5'SS: alternative 5' splice site; MXE: mutually exclusive exon; RI- retained intron. % skipped and included DSEs are indicated.
- (B) Gene Set Enrichment Analysis for DSEs detected in SF-OE MCF-10A day-8 acini showing the top 10 Hallmark gene sets.
- (C) Shared DSGs in SF-OE MCF-10A day-8 acini for each indicated SF pair. Bubble size is proportional to the number of shared DSGs and color indicates  $P$ -value. See also [Table S3G](#).
- (D) % of DSEs that affect a region containing an annotated protein domain (*i.e.*, IPRO ID) for both unique and shared DSEs in SRSF4-, SRSF6- and TRA2 $\beta$ -OE MCF-10A day-8 acini. Fisher's exact test  $P$ -value is indicated. See also [Table S3H](#).
- (E-G) Similarities and differences in differentially expressed genes (DEGs).
- (E) Volcano plots depicting  $\log_2$ fold gene expression changes ( $\log_2\text{FC}$ ) and significance as  $-\log_{10}(\text{q-value})$  for each in SF-OE vs. control MCF-10A day-8 acini. Significant genes are shown in blue, non-significant in grey. See also [Table S4](#).
- (F) Overlap in DEGs in SF-OE MCF-10A day-8 acini for each indicated SF pair. Bubble size is proportional to the number of shared differentially expressed genes and color indicates  $P$ -value. See also [Table S4](#).
- (G) Gene Set Enrichment Analysis for DEGs detected in SRSF4-, SRSF6-, and TRA2 $\beta$ -OE MCF-10A day-8 acini showing the top biological functions. See also [Table S4](#).

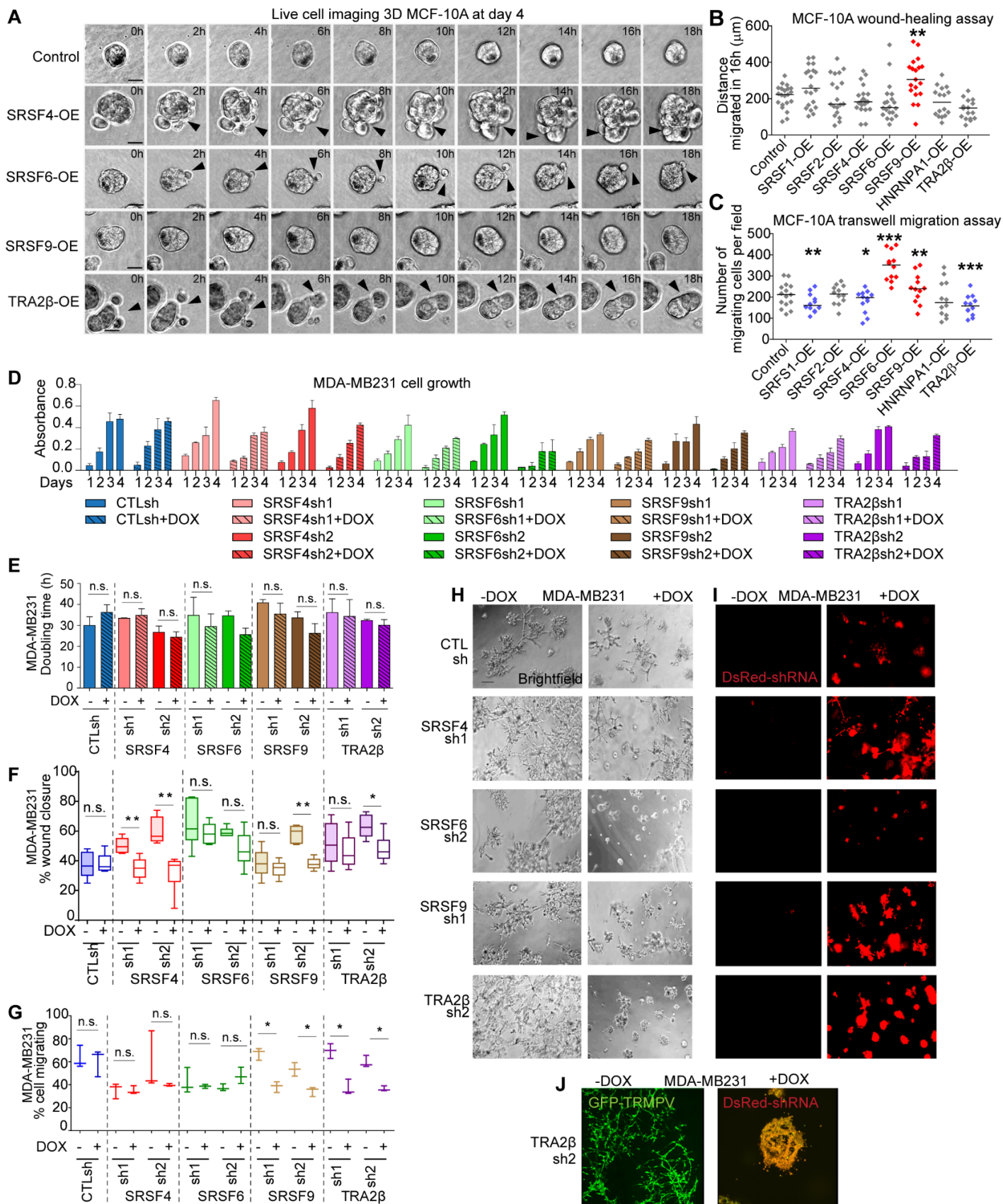


**Figure S5. SF levels affect cell migration and invasion** (related to [Figure 5](#)).

(A-C) SF-OE promotes different types of cell movement in human mammary MCF-10A cells.

(A) Representative images of intra-acinar cell movement of control or SF-OE MCF-10A day-4 acini imaged during an 18h period by live cell microscopy. Cells moving abnormally outside or inside the acini are indicated by arrowheads (scale bar: 50μm).

**(B-C)** Quantification of control or SF-OE MCF-10A cell migration in a wound-healing assay (B), or in transwell migration assays (C). The plot shows the distribution and the median (horizontal line) for each condition ( $n \geq 4$  biological replicates; t-test  $***P < 0.0001$ ,  $**P < 0.005$ ,  $*P < 0.05$ ).

**(D-J)** SF levels affect cell invasion in TNBC MDA-MB231 cells.

**(D)** Relative cell number measured by MTT assay at days 1 to 4 in CTLsh or SFsh MDA-MB231 cell lines +/-DOX ( $n=3$  biological replicates; mean +/-SD).

**(E)** Cell doubling time as calculated from (D). ( $n=3$  biological replicates; mean  $\pm$ SD; t-test, n.s. not significant).

**(F-G)** Migration of CTLsh or SFsh MDA-MB231 cells +/-DOX in 2D wound-healing (F) or 2D transwell assay (G) ( $n \geq 3$ ; t-test,  $**P < 0.005$ ,  $*P < 0.05$ ).

**(H-I)** Representative images of CTLsh or SFsh MDA-MB231 cells, grown in 3D +/-DOX, imaged at day 8 with brightfield (H) and fluorescence (I) (scale bar:  $100\mu\text{m}$ ). Cell expressed DsRed once the shRNA is induced.

**(J)** Maximal projection reconstruction of representative Z-stack fluorescent confocal images of TRA2 $\beta$ sh2 MDA-MB231 cells, grown in 3D +/-DOX, imaged at day 8 for GFP and DsRed expression (scale bar:  $100\mu\text{m}$ ). Cells that integrate the shRNA-containing TRMPV plasmid constitutively express GFP, as well as DsRed once the shRNA is expressed.

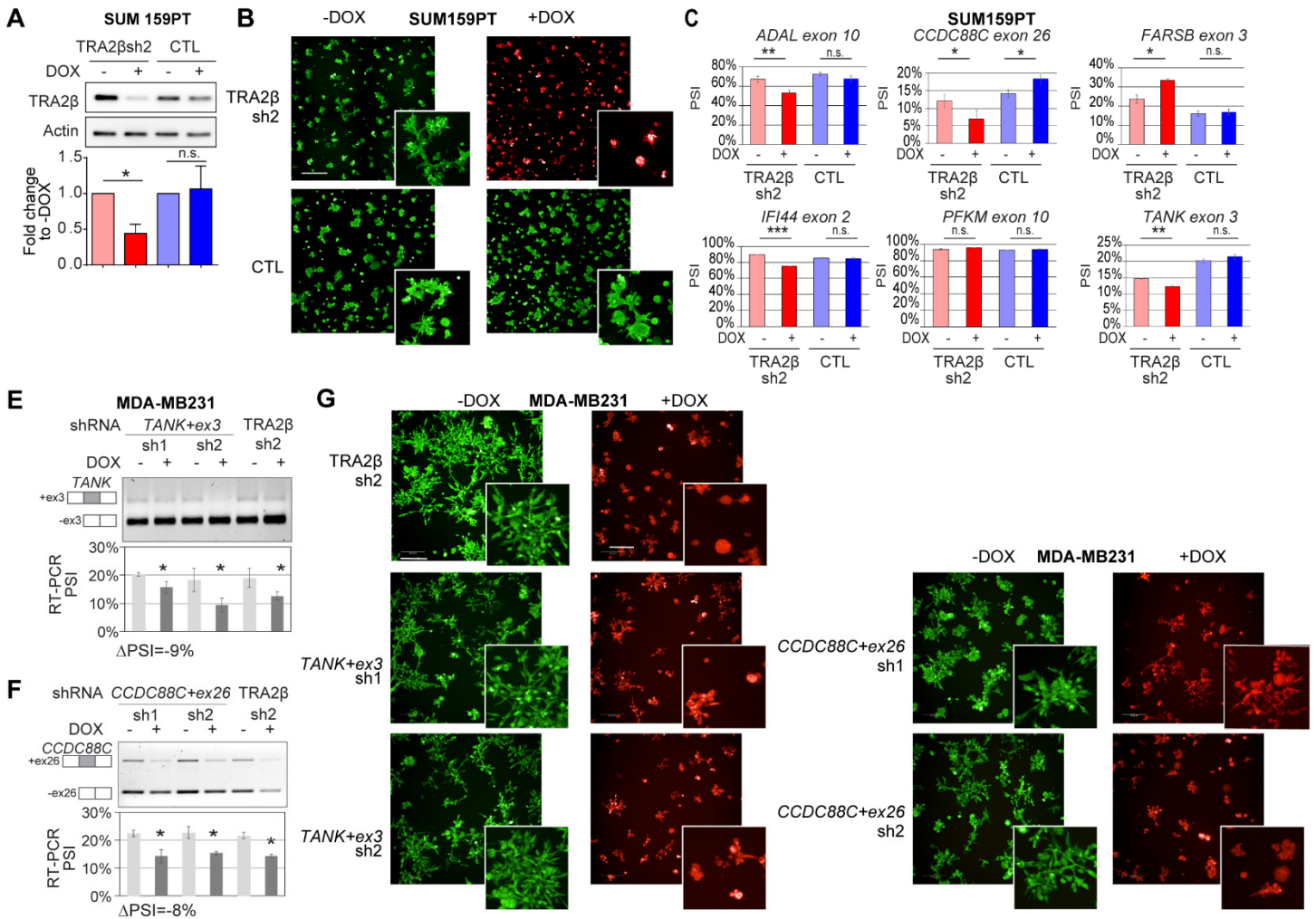


**Figure S6. TRA2β-KD and TRA2β-regulated spliced isoforms affect cell invasion in TNBC cells** (related to [Figure 5](#) and [6](#)).

**(A-C)** TRA2β-KD affects cell invasion and spliced isoforms in SUM159PT TNBC cells.

**(A)** TRA2β protein expression in TRA2βsh2 SUM159PT cells +/-DOX compared to control. TRA2β levels are quantified 72h after 1X DOX treatment by western blotting using a TRA2β-specific antibody and normalized to actin. % TRA2β expression +DOX is normalized to -DOX (n=3; mean±SD; \**P*<0.05).

**(B)** Maximal projection reconstruction of representative Z-stack fluorescent confocal images of TRA2βsh2 and control SUM159PT cells, grown in 3D +/-DOX, imaged at day 5 for GFP and DsRed expression (scale bar: 500μm). Maximal projection images are composed of 30-35 Z-stack images spaced every 55 μm. At least 15 fields are imaged per condition. Cells that integrate the shRNA-containing TRMPV plasmid constitutively express GFP, as well as DsRed once the shRNA is expressed. Control cells are stained with calcein-AM live-cell dye.

**(C)** RT-PCR validations of selected DSEs in TRA2βsh2 SUM159PT and control cells ±DOX, as in [Figure 6D](#). (n=3; mean±SD; t-test, \*\*\**P*<0.0005; \*\**P*<0.005; \**P*<0.05; n.s. not significant).

**(E-G)** TRA2β-regulated isoforms of *CCDC88C* and *TANK* affect cell invasion and morphogenesis of MDA-MB231 TNBC cells.

**(E,F)** DOX-inducible shRNAs targeting mRNA isoforms of *TANK+ex3* (E) or *CCDC88C+ex26* (F), decrease the expression of exon-containing isoforms in 3D MDA-MB231 cells grown on day 8 as detected by RT-PCR, and compared to TRA2βsh2. A representative gel is shown, along with isoform structures. PSI values for all samples and ΔPSI for significant samples are calculated from RT-PCR for +DOX vs. -DOX (n=3; mean±SD; t-test, \**P*<0.05).

**(G)** Maximal projection reconstruction of representative Z-stack fluorescent confocal images of *TANK+ex3sh* or *CCDC88C+ex26sh* MDA-MB231 cells grown in 3D, ±DOX, imaged at day 6 for GFP and DsRed expression (scale bar: 200μm), and compared to TRA2βsh2 MDA-MB231 cells. Maximal projection images are composed of 30-35 Z-stack images spaced every 55 μm. At least 15 fields are imaged per condition. Cells constitutively express GFP, whereas DsRed is expressed with the shRNA is activated.

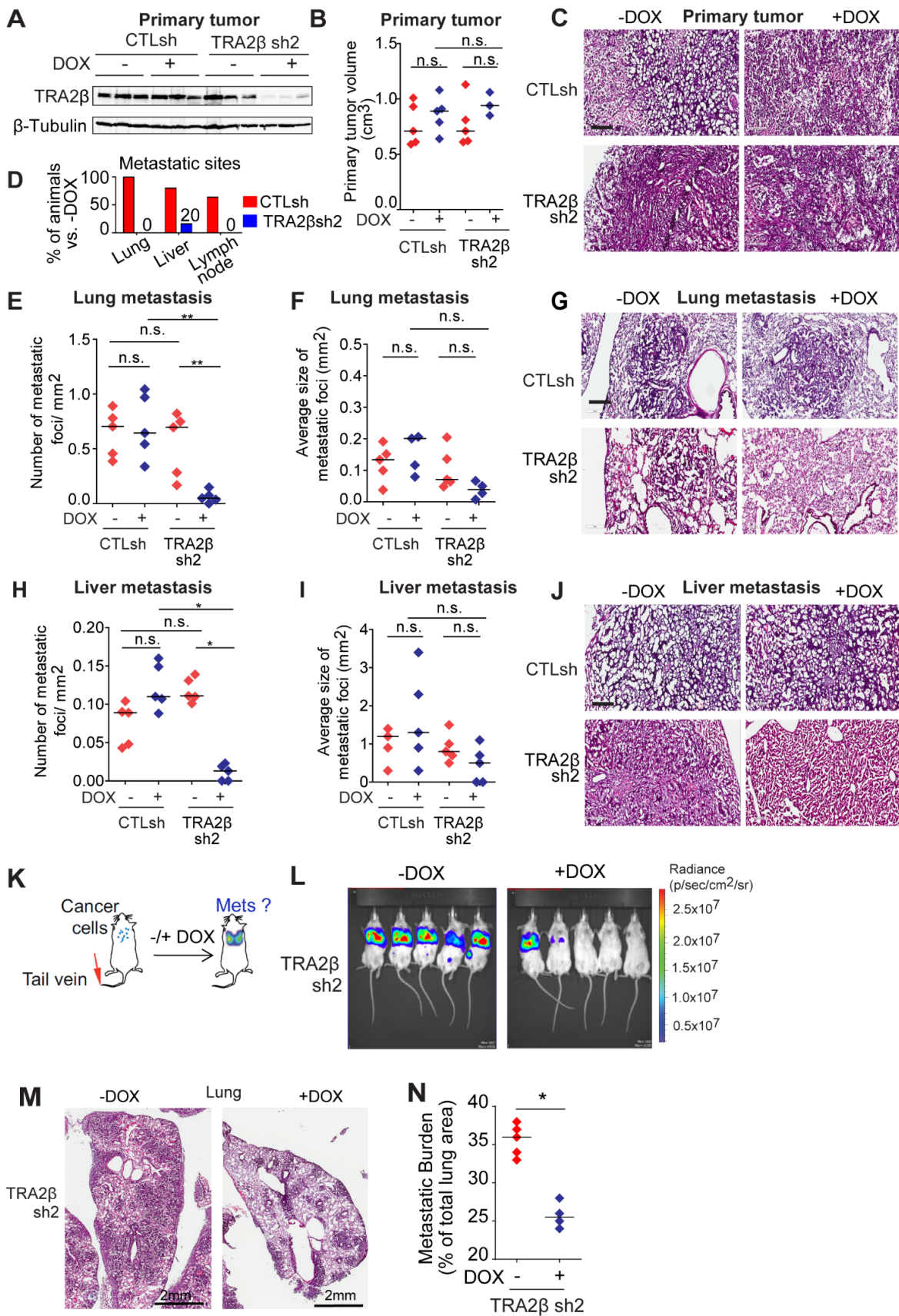


**Figure S7. TRA2 $\beta$ -KD decreases metastatic burden in TNBC metastasis models (related to Figure 7).**

**(A-J)** TRA2 $\beta$ -KD decreases metastatic burden in a spontaneous metastasis model of TNBC.

**(A)** TRA2 $\beta$  levels are assessed by western blot in primary tumors from animals injected with CTLsh or TRA2 $\beta$ sh2 MDA-MB231 cells  $\pm$ DOX. DOX induces shRNA expression.

- (B,C)** Primary tumor size is measured at necropsy in CTLsh and TRA2 $\beta$ sh2 tumors (B) and representative H&E-stained tumor sections are shown (scale bar: 1mm) (C) at 8 weeks post-injection.
- (D)** % of animals that exhibited macro-metastases at different organ sites in animals injected with CTLsh and TRA2 $\beta$ sh2 MDA-MB231 cells  $\pm$ DOX is assessed at necropsy at 8 weeks post-injection.
- (E-J)** Lung (E-G) and liver (H-J) metastasis in animals injected with CTLsh or TRA2 $\beta$ sh2 MDA-MB231 cells  $\pm$ DOX are scored through the whole organ using multiple H&E sections evenly distributed every 2mm. The number of metastatic foci per mm<sup>2</sup> (E, H) and the average size of metastatic foci (F, I) are quantified ( $n \geq 4$ ; t-test \*\* $P < 0.001$ , \* $P < 0.01$ , n.s. not significant). Representative H&E-stained frozen tumor sections are shown (scale bar: 1mm) (G, J).
- (K-N)** TRA2 $\beta$ -KD decreases lung tumors formation in an intravenous experimental metastasis model of TNBC.
- (K)** MDA-MB231 TRA2 $\beta$ sh2 cells are injected into the tail vein of NSG mice; metastases are monitored by bioluminescence imaging and histopathology.
- (L)** Bioluminescence detection of metastasis in mice injected with MDA-MB231 TRA2 $\beta$ sh2 cells  $\pm$ DOX at 6 weeks post-injection. DOX induces shRNA expression.
- (M)** Representative H&E pictures from lung sections of mice injected with MDA-MB231 TRA2 $\beta$ sh2 cells  $\pm$ DOX at 6 weeks post-injection (scale bar: 2 mm). Metastases are scored through the whole organ using sections evenly distributed every 2mm and quantified in D.
- (N)** Quantification of metastasis burden (% of metastatic organ area relative to the whole organ area) in mice injected with MDA-MB231 TRA2 $\beta$ sh2 cells  $\pm$ DOX at 6 weeks post-injection ( $n \geq 4$ ; t-test, \* $P < 0.02$ ).